Crystal Aging and Crystal Habit of Terephthalic Acid

Michael Saska
Audubon Sugar Institute
and Department of Chemical Engineering
Louisiana State University
Baton Rouge, LA 70803

A. S. Myerson
Department of Chemical Engineering
Polytechnic University
Brooklyn, NY 11201

Introduction

The aging of crystals comprises all structural changes that occur in crystals after nucleation and crystal growth have occurred. There are several different phenomena that fall under the general classification of aging. The best known of these is Ostwald ripening, which refers to the tendency of smaller particles dispersed in a saturated solution to dissolve and their material to be deposited on the larger particles. A type of aging different from Ostwald ripening involves the tendency of imperfect crystals placed in their own saturated solution to perfect themselves. This type of aging has been extensively studied by Kolthoff and coworkers (1938a,b,c), who studied the aging of precipitates that had been formed rapidly. More recently Gaines and Myerson (1982, 1983) examined the aging of terephthalic acid (TPA) in a batch suspension crystallizer. This experiment showed that the initial TPA particles, which had a globular appearance and a mean size of 1×10^{-4} m, transformed into larger needle crystals. In addition to the habit change, the purity of the crystals increased in these experiments.

It is the purpose of this work to examine in detail the aging of terephthalic acid in order to better understand the mechanism of the process and to evaluate crystal aging as a possible purification technique.

Characterization of Commercial TPA Samples

Terephthalic acid is typically produced by the oxidation of paraxylene. The impurities found in TPA manufactured in this way can be classified as:

1. Reaction intermediates
2. Secondary reactants
3. Inorganic material

The reaction intermediates formed are the compounds *p*-tolualdehyde, *p*-toluic acid, and 4-carboxybenzaldehyde (4-CBA). The main impurity found in TPA is 4-CBA, usually present in a concentration of up to 500 ppm. Inorganic impurities (such as cobalt) which catalyze the oxidation reaction, are often also present in concentrations up to 500 ppm. The impurities mentioned cause color in the product polymer and sometimes hinder polymerization.

Seven commercial samples of TPA were supplied by manufacturers for these studies. The samples were initially examined by scanning electron microscopy (SEM) and optical microscopy for estimation of the average particle size and observation of the crystal habit. The concentrations of the impurities 4-CBA and cobalt were also measured. The average particle sizes of the samples appear in Table 1 along with the 4-CBA and cobalt con-

Table 1. Average Size and Purity of Commercial TPA Samples

Sample	Avg. Size $m \times 10^{-6}$	4-CBA Conc. ppm	Cobalt Conc. ppm
A	100	24	1–3
B	30	2,784	—
C	80	130	—
D	150	220	5
E	40	3,902	404
F	10	4,957	35
G	1 and 30 (bimodal)	7,514	65

Correspondence concerning this paper should be addressed to A. S. Myerson.

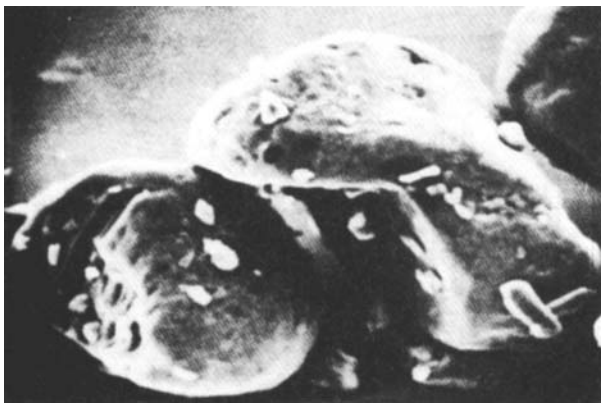

Figure 1. SEM photograph (×500) of typical commercial TPA sample.

centrations. These results show significant variations in purity and average size. Particles in all samples except *A* and *C* were mostly spherical, without plane surfaces and crystallographic angles. Sample *C*, however, was composed of regular single crystals of approximately 50 micron (μm) size and regular shape. By checking with the manufacturer it was determined that sample *C* had undergone a kind of aging purification step after formation in the reactor, thus accounting for its shape. An SEM of a typical sample is shown in Figure 1. In Figure 2, an example is given of a needle crystal obtained on aging TPA in a batch suspension crystallizer (Myerson and Saska, 1984) at 200°C for 6 h.

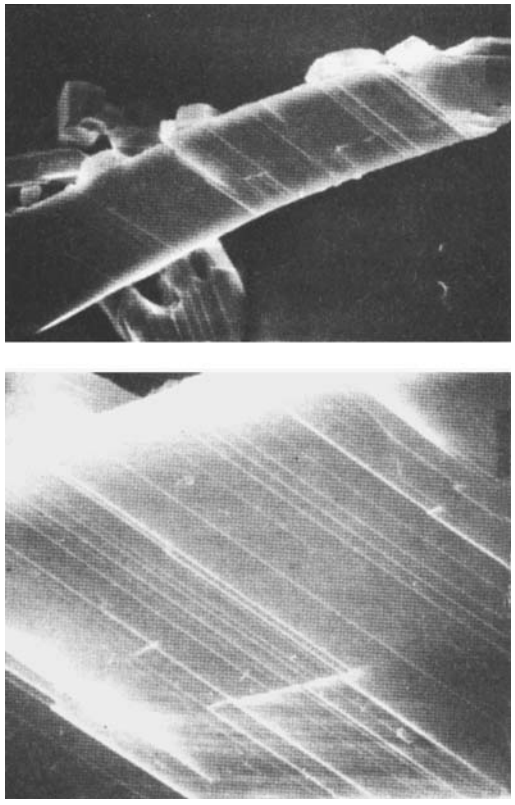

Figure 2. SEM photograph of typical aged TPA crystal.
Top, Segmentation visible approximately perpendicular to growth direction (×200).
Bottom, detailed view of segmentation (×1,000).

TPA Crystal Structure

The drastic change in crystal habit observed during the aging of TPA suggests the possibility of a polymorphic phase transformation. Bailey and Brown (1967) reported the existence of two polymorphic forms, I and II, of TPA and measured their unit cell parameters. In more recent work (Saska and Myerson, 1985; Myerson and Saska, 1984) fresh and aged TPA was examined by X-ray diffraction. The results indicated that only form I was present. It was decided to further pursue this area to determine at what conditions, if any, polymorph form II could be obtained.

TPA samples obtained from commercial manufacturers along with samples prepared by aging and recrystallization under a wide variety of conditions (Saska, 1984; Gaines and Myerson, 1982, 1983) were evaluated by X-ray powder diffraction. A total of 50 samples were examined and the resulting patterns compared to theoretical patterns calculated from the single-crystal data on both polymorphs of Bailey and Brown (1967). All of the observed patterns conformed to the three major reflections reported for TPA polymorph I. These results are summarized in Table 2; details may be found in Saska (1984).

TPA polymorph II was not evident in the powder diffraction patterns; however, if one of the components in a mixture is present in only a small concentration, its presence may not be apparent by visual estimate of the powder diffractograms. Pattern-fitting structure-refinement techniques (Rietveld, 1967; Wiles

Table 2. TPA Crystal Structure

	Single-Crystal and Powder X-ray Data		
	Form I		Form II
	This work	Bailey and Brown (1967)	Bailey and Brown (1967)*
a, Å	7.736	7.730	9.54
b	6.444	6.443	5.34
c	3.7504	3.749	5.02
α, °	91.51	92.75	86.95
β	109.12	109.15	134.56
γ	95.77	95.95	94.80

	Position (28°) of the Three Major Reflections	
	Form I	Form II
This work, calc. from single-crystal data**	17.39	—
	25.20	—
	27.79	—
Bailey and Brown (1967)†	17.33	16.67
	25.26	25.25
	27.57	30.27
This work, obs., avg. of 46 polycrystalline patterns	17.37 ± 0.07	—
	25.19 ± 0.07	—
	27.86 ± 0.08	—
Powder Diffraction File‡	17.36	—
	25.23	—
	27.97	—

*Initial triclinic cell where the molecule is placed along the *a* direction
**Using the 7.736, 6.444, 3.7504 Å axes
†Using the 7.730, 6.443, 3.749 Å axes
‡Joint Committee on Powder Diffraction Standards (1976)

and Young, 1981) utilize the whole pattern including the background signal to refine the structural parameters of substances not available in single-crystal form. The refinement accuracy is comparable to average single-crystal results. No evidence of form II was obtained. It was therefore concluded that the crystal aging observed was not the result of a polymorphic transformation.

Calculated and observed habit of TPA crystals

It has become generally accepted that crystal shapes are determined by the kinetic processes of growth. Hartman and Bennema (1980) and Hartman (1980a,b) have demonstrated a correlation between the growth velocity of a face and its attachment energy. Where the BCF crystal growth model applies, the linear growth velocity R of a face $(hk1)$ can be written (for low σ) as:

$$R_{hkl} \sim \frac{\sigma^2 \exp(AE_{hkl})}{(1 - BE_{hkl})\sqrt{2AE_{hkl}}} \tanh\left[\frac{(1 - BE_{hkl})\sqrt{2AE_{hkl}}}{\sigma \exp(AE_{hkl})}\right] \quad (1)$$

where σ is the supersaturation, A and B are constants, and E_{hkl} is the attachment energy per mole of the $(hk1)$ face, which is equal to the energy released per mole when a crystal slice is deposited on the face $(hk1)$. For a narrow range of attachment energies, Eq. 1 indicates that $R_{hkl} \sim E_{hkl}$. The surface energy of a face, e_i, can be related to the Gibbs free energy of the surface, γ_i, by the relation

$$e_i = \gamma_i - T\left(\frac{\partial \gamma}{\partial T}\right)_p \quad (2)$$

When the derivative of surface free energy with respect to temperature is small, Eq. 2 can be written as:

$$e_i = \gamma_1 \quad (3)$$

The surface energy is then assumed to be proportional to E_{hkl}, which can be calculated by the summation of interatomic interactions over a sufficient distance. Calculations of this type have appeared in the literature for a variety of substances, including naphthalene, SnI_4, sulfur, and corundum (Hartman, 1980a,b). Theoretical growth shapes calculated assuming $R_{hkl} \sim E_{hkl}$ agree quite well with the experimentally determined shapes. Results obtained from corundum (Hartman, 1980b) lead to the conclusion that the actual shapes were affected by specific adsorption.

Values of the surface energies of individual crystallographic faces of crystalline TPA were calculated using the potential functions of Kitaigorodski (1973) and Brant and Flory (1965). These surface energies were then employed with a computer program previously developed (Saska and Myerson, 1983) to calculate the position of all crystallographic planes specified and to project the resulting shape on an arbitrary plane. The computer program consists of the following operations:

1. Set up the analytical equation for all planes specified.
2. Calculate the position of points resulting from intersection of all planes.
3. Discard the points lying outside the crystal boundary.
4. Decide whether a plane is visible in the required rotation.
5. Connect the corners of the crystal.

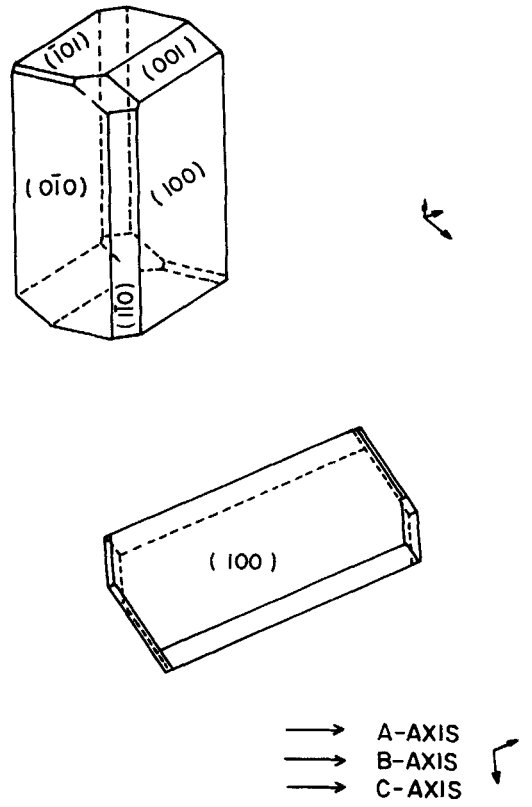

Figure 3. Calculated growth form of TPA crystal using Donnay-Harker condition.

Crystal shapes were also calculated based on the Donnay-Harker (1937) law (where the growth rate of face i is inversely proportional to the interplanar spacing of the crystallographic plane i) and the equilibrium (Wulff) condition (where the growth rate, R_i, is proportional to γ_i, the surface Gibbs free energy of face i). The resulting crystal shapes are shown in Figures 3–5.

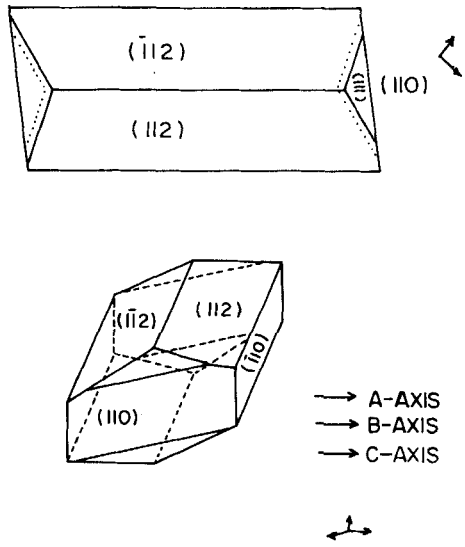

Figure 4. Calculated Equilibrium form of TPA crystal using Wulff condition and Kitaigorodski potential function.

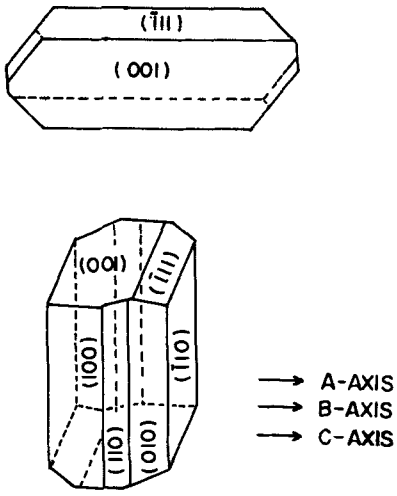

Figure 5. Calculated growth form of TPA crystal using Hartman condition and Kitaigorodski potential function.

The habit of a typical aged TPA crystal (Saska, 1984; Gaines and Myerson, 1982) viewed along its long dimension is shown in Figures 2 and 6. Interfacial angles were measured from SEM photographs for 10 crystals and averaged to produce the typical habit given in Figure 7. Comparison with the calculated habits shows a fair agreement between the calculated Hartman habit and the actual habit. This can be seen by comparing the projection along the long (c axis) dimensions of the calculated Hartman crystal shown in Figure 8 with the average observed crystal shown in Figure 7. Comparison of the aged crystals with the Donnay-Harker and Wulff habits showed little agreement. This result indicates that aging might be the result of a BCF-type growth mechanism.

Aging in microsystems

In order to further study the habit transformation that accompanies crystal aging, microscopic aging experiments were designed and performed. In these experiments a small amount of the crystal-liquid mixture was enclosed in a glass capillary capable of withstanding pressures up to 500 psi (3.4 MPa). The capillary was sealed at both ends and placed on the hot stage of a Leitz microscope. This arrangement allowed direct observation of aging at elevated temperatures. In addition, the small volume

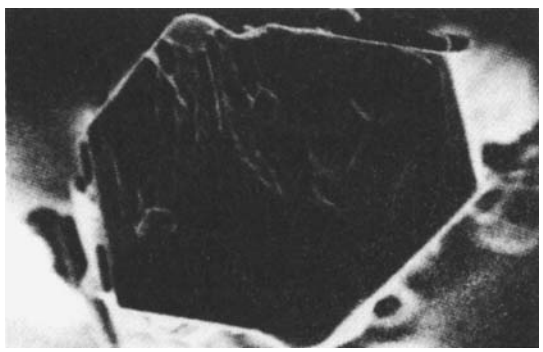

Figure 6. Rod TPA crystal (×400) viewed along its long dimension.
End of crystal is faceted with apparent growth instabilities.

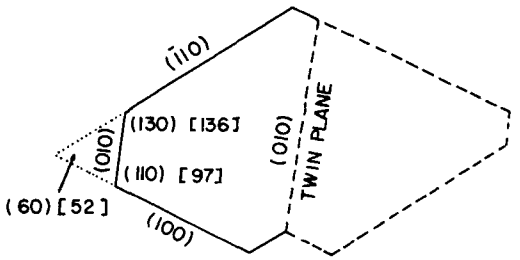

Figure 7. Contour of typical TPA crystal viewed along its long dimension.
(Average measured interfacial angles)
[Calculated Crystallographic Angles.]

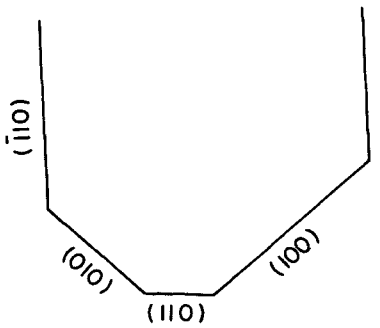

Figure 8. Contours along c crystallographic axis of crystal form predicted using Hartman condition.

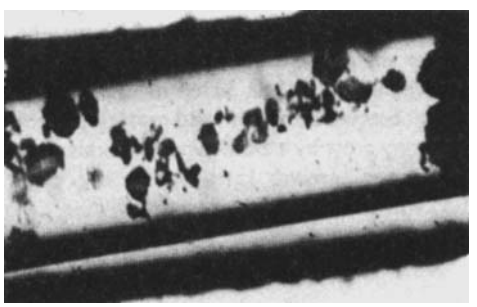

Figure 9. Aging of TPA in a glass capillary.

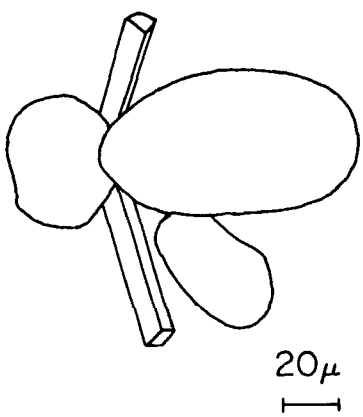

Figure 10. Drawing of a pattern observed on aging TPA in a glass capillary.

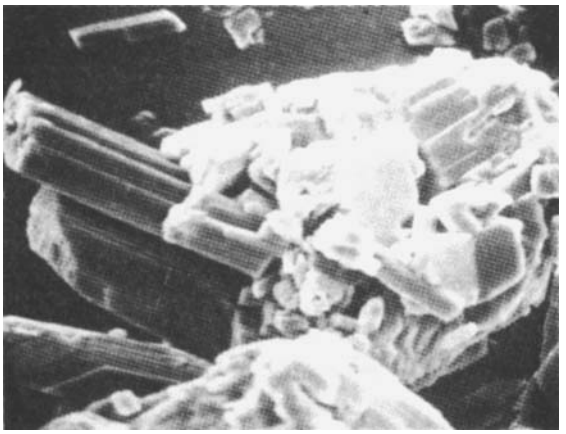

Figure 11. Aged TPA particle (×820) after 60 min at 207°C in a glass capillary.

of the system allowed for much more rapid heating and cooling at the beginning and end of each experiment as well as precise temperature control. Typical results are shown in Figures 9 and 10. These results show rod-shaped faceted particles that have nucleated and grown on the original globular TPA particles. An SEM photograph of this appears in Figure 11.

Discussion

The habit change observed during the aging of terephthalic acid appears to be the result of new rodlike crystals nucleating and growing on the surface of the globular particles initially present. The nucleation and growth of the new crystals indicates that a finite supersaturation must exist which may be the result of temperature and concentration fluctuations. The agreement between the calculated habits based on the Hartman kinetic model and the observed habits of aged crystals suggests that the aged crystals may grow by a BCF-type mechanism. Direct measurement of crystal growth rates during the aging of terephthalic acid will be required, however, to further elucidate the crystal growth mechanism.

Literature cited

Bailey, M., and C. J. Brown, "The Crystal Structure of Terephthalic Acid," *Acta Cryst.*, **22,** 387 (1967).

Brant, D. A., and P. J. Flory, "The Role of Dipole Interactions in Determining Polypeptide Configuration," *J. Am. Chem. Soc.*, **87,** 663 (1965).

Donnay, J. D. H., and D. Harker, "A New Law of Crystal Morphology Extending the Law of Bravais," *Am. Mineralogist*, **22,** 446 (1937).

Gaines, S., and A. S. Myerson, "Removal of Impurities through Crystal Aging," *AIChE Symp. Ser. No. 215*, **78,** 42 (1982).

Gaines, S., and A. S. Myerson, "The Agglomeration and Aging of Terephthalic Acid Particles," *Particulate Sci. Technol.*, **1,** 409 (1983).

Hartman, P., "The Attachment Energy as a Habit-Controlling Factor. II: Application to Anthracene, Tin-Tetraiodide and Orthorhombic Sulfur, *J. Cryst. Growth*, **49,** 157 (1980a).

———, "The Attachment Energy as a Habit-Controlling Factor. III: Application to Corundum," *J. Cryst. Growth*, **49,** 166 (1980b).

Hartman, P., and P. Bennema, "The Attachment Energy as a Habit-Controlling Factor. I: Theoretical Consideration," *J. Cryst. Growth*, **49,** 145 (1980).

Kitaigorodski, A. I., *Molecular Crystals and Molecules*, Academic Press, New York, 388 (1973).

Kolthoff, I. M., and G. E. Noponen, "Studies on Aging of Fresh Precipitates. XVI: The Distribution Coefficient of Choromate Ions between Barium Sulfate and Aqueous Solutions," *J. Am. Chem. Soc.*, **60,** 39 (1938b).

———, "Studies on Aging of Fresh Precipitates. XVII: The Equilibrium between Mixed Crystals of Barium-Lead Sulfate and Solutions," *J. Am. Chem. Soc.*, **60,** 197 (1938a).

Kolthoff, I. M., and W. von Fisher, "Studies on Aging Precipitates. XXIV: The Apparent Effect of Filtration upon the Aging of Fresh Lead Sulfate," *J. Am. Chem. Soc.*, **61,** 191, (1938c).

Myerson, A. S., and M. Saska, "Formation of Solvent Inclusions in Terephthalic Acid Crystals," *AIChE J.*, **30,** 865 (1984).

Rietveld, H. M., "Line Profiles of Neutron Powder-Diffraction Peaks for Structure Refinement," **22,** 151 (1967).

Saska, M., "Crystallization of Terephthalic Acid," Ph.D. Diss., Georgia Inst. Technol., Atlanta (1984).

Saska, M., and A. S. Myerson, "The Theoretical Shape of Sucrose Crystals from Energy Calculations," *J. Cryst. Growth*, **61,** 546 (1983).

———, "Polymorphism and Aging in Terephthalic Acid," *Cryst. Res. Technol.*, **20,** 201 (1985).

Wiles, B. B., and R. A. Young, *J. Applied Cryst.*, **14,** 149 (1981).

Manuscript received Mar. 19, 1986, and revision received July 10, 1986.